Available online at www.sciencedirect.com
ScienceDirect
Journal of the European Ceramic Society 30 (2010) 3167–3171
www.elsevier.com/locate/jeurceramsoc

Magnetic properties and remanence analysis in permanently magnetic $BaFe_{12}O_{19}$ foams

Ugur Topal [a,*], Halil I. Bakan [b]

[a] TUBİTAK, UME (National Metrology Institute), P.K. 54, Gebze 41470 - Kocaeli, Turkey
[b] TUBİTAK, MAM, Material Institute, P.K. 21, Gebze 41470 - Kocaeli, Turkey

Received 2 April 2010; received in revised form 4 June 2010; accepted 16 June 2010
Available online 11 July 2010

Abstract

In the present study, magnetic properties of barium ferrite foams were investigated. We especially examine the effects of porosity on interparticle interactions and remanence properties of these materials. It was observed that magnets become harder with porosity. On the other hand, saturation magnetization decreases slightly. Existence of porosities increases the strength of demagnetising-like interactions of neighboring particles.

PACS: 61.43.Gt; 81.05.Rm; 75.50.Ww; 75.60.Ej

Keywords: Porous materials; Permanent magnets; Exchange coupling; Remanence properties

1. Introduction

M-type barium ferrite with hexagonal structure ($BaFe_{12}O_{19}$) is a well known high-performance permanently magnetic material, due to its large magnetocrystalline anisotropy, high Curie temperature, relatively large magnetization, excellent chemical stability and corrosion resistivity.[1,2] These features make their applications possible in different areas such as permanent magnets, microwave devices and perpendicular magnetic recording media. Recently, we have achieved to fabricate hard magnetic barium ferrite having a foamy structure and preliminary results were published elsewhere.[3] These materials seem to find new application areas in industry mainly due to their light weights and possibility of filling the pores by other materials having different physical property, such as semiconducting, superconducting and polymeric materials. That is, hybrid structures can be formed. In the present study, we examine the magnetic properties of barium ferrite foams extensively. We especially focus on understanding the role of porosity on remanence properties. For this purpose, three samples were synthesized at same furnacing conditions but different pore dimensions and concentrations.

Investigation and understanding the strength of intergrain or interparticle exchange couplings has attracted much attention in the field of magnetism in order to interpret magnetic parameters of the materials which show giant magnetoresistance, soft or hard magnetic properties, etc.[4–8] For instance, exchange couplings between grains tend to reduce the storage density of magnetic recording media, and hence the isolation of particle is needed.[4] On the other hand, exchange couplings are desired to obtain high-performance permanent magnets.[9,10] In this study, the influence of porosity on interparticle interactions or exchange couplings, which affect the remanence properties, were examined by the use of remanence relationship

$$M_D(H) = M_R(H_{\max}) - 2M_R(H),$$

derived by Wohlfarth and holds for noninteracting particles.[11] In this equation, $M_D(H)$ is demagnetization remanence and $M_R(H)$ is isothermal magnetization remanence. Deviation from this equation is explained by existence of particle interactions. For interacting particles, the equation above was modified by Kelly et al.[12] as

$$\delta M(H) = m_D(H) - (1 - 2m_R(H)),$$

which gives the sign and the relative strength of the interactions. Here $m_R(H)$ and $m_D(H)$ are the remanences normalized to the saturation remanence value $M_R(H_{\max})$.

* Corresponding author.
E-mail addresses: ugur.topal@ume.tubitak.gov.tr (U. Topal), Halil.Bakan@mam.gov.tr (H.I. Bakan).

0955-2219/$ – see front matter © 2010 Elsevier Ltd. All rights reserved.
doi:10.1016/j.jeurceramsoc.2010.06.008

Table 1
Cell size, corresponding diameters of the cells and total porosity of the used polyurethane foams (PU) as given by the manufacturer.

Pore size per inch (ppi)	Corresponding mean cell diameter in mm	Total porosity of polyurethane foams [vol%]
30	1.8–2	98.4
80	0.4–0.5	97.3

2. Experimental

Barium carbonate ($BaCO_3$) and iron oxide (Fe_2O_3) were used as the starting materials. Required amounts of $BaCO_3$ and Fe_2O_3 powders of high purity (99%) were weighed and mixed at Fe/Ba atomic ratio of 10.5 by using a turbula mixer for 3 h. The powder mixture was divided into the two lots. The first lot was used for preparation of powder slurry for synthesis of $BaFe_{12}O_{19}$ foams. The other lot was used to make compact samples. Open celled $BaFe_{12}O_{19}$ foams were produced by replication method using reticulated polyurethane sponges as templates. PEG (polyethylene glycol) and carboxy methyl cellulose (CMC) were used as binders for the preparation of powder slurry. First PEG and CMC were stirred in distilled water at temperature of 75 °C for 1 h in order to obtain solution. Then, the mixture of Fe_2O_3 and $BaCO_3$ was subsequently added to the solution and stirred for 3 h in order to produce the water based slurry with solid content of 50 wt%. Polyurethane sponge samples with cell sizes of 30 and 80 pores per inch were used in this study. Table 1 shows the corresponding cell diameters and total porosity of the used polyurethane sponges as given by the manufacturer. Polyurethane sponge samples were dipped into the slurry. This dipping process was repeated until all the struts of polyurethane sponge were covered with slurry. The excess slurry was removed by passing the samples through a set of rotating rollers at a fixed distance. After passing through the rollers the samples were placed in a drying oven featuring both temperature and humidity control. After drying, the polyurethane sponge were removed from the coated sponge samples by a pyrolysis step in air using a slow heating rate (1 °C/min to 650 °C) and then the samples were heated at a rate of 10 °C/min to the sintering temperature of 1400 °C and held at this temperature for 2 h. The compact samples were produced from the second lot mentioned above. The powder mixture was pelletized at 250 MPa. Then the pellets were sintered at 1400 °C for 2 h.

Magnetic properties of the samples were examined at room temperature using a vibrating sample magnetometer (VSM) with a maximum applied field of 15 kOe. Isothermal magnetization remanence, $M_R(H)$, was measured on thermally demagnetized samples. A small field is applied, then removed and the remanent magnetization is measured. The remanence was measured as a function of increasing field until saturation remanence had been reached. Demagnetization remanence, $M_D(H)$, was measured as follows: the sample is initially saturated in one direction and then a small reverse field is applied, removed and the remanence is measured. This process is repeated until negative saturation remanence was observed. It is also important to note that remanences were measured after no change on their values are seen (i.e. let enough time for magnetic relaxation).

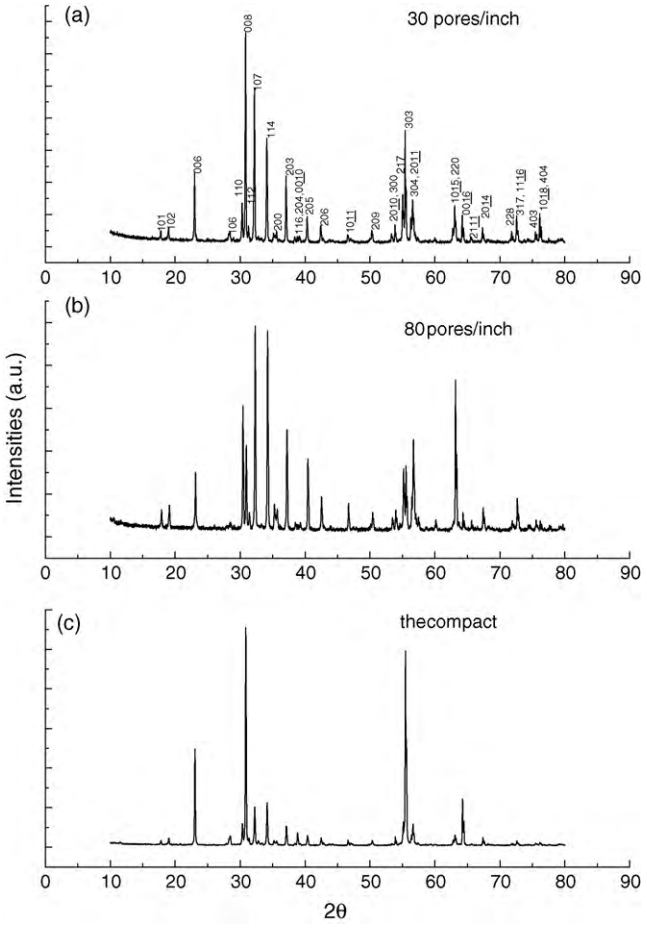

Fig. 1. (a–c) The X-ray diffraction patterns of the foam and the compact samples.

For microstructural analysis, samples were examined in a scanning electron microscope. X-ray diffraction analysis was performed in order to determine the phases present in the samples.

3. Results and discussion

Fig. 1 shows the XRD patterns of the samples including different amounts of pores ((a) 30 pores/in., (b) 80 pores/in. and (c) the compact sample). Positions of the peaks are same in the samples examined and all diffraction peaks appeared were indexed to the $BaFe_{12}O_{19}$ phase. No secondary phases were detected. Relative intensities of the peaks show difference, which may be due to the different crystallographic orientation of the samples. Well-defined sharp peaks indicate the good crystalline quality of these samples.

Fig. 2 shows SEM micrographs of the compact and the foam samples. All samples consist of heterogeneously distributed grain sizes ranging between 10 μm and 100 μm, which is mainly due to the requirement of high sintering temperature (@ 1400 °C). Almost all grains of the studied samples have hexagonal shapes as seen in Fig. 2(c) (see also Ref. 3 for SEM images of the sample with 30 pores/in. taken at higher magni-

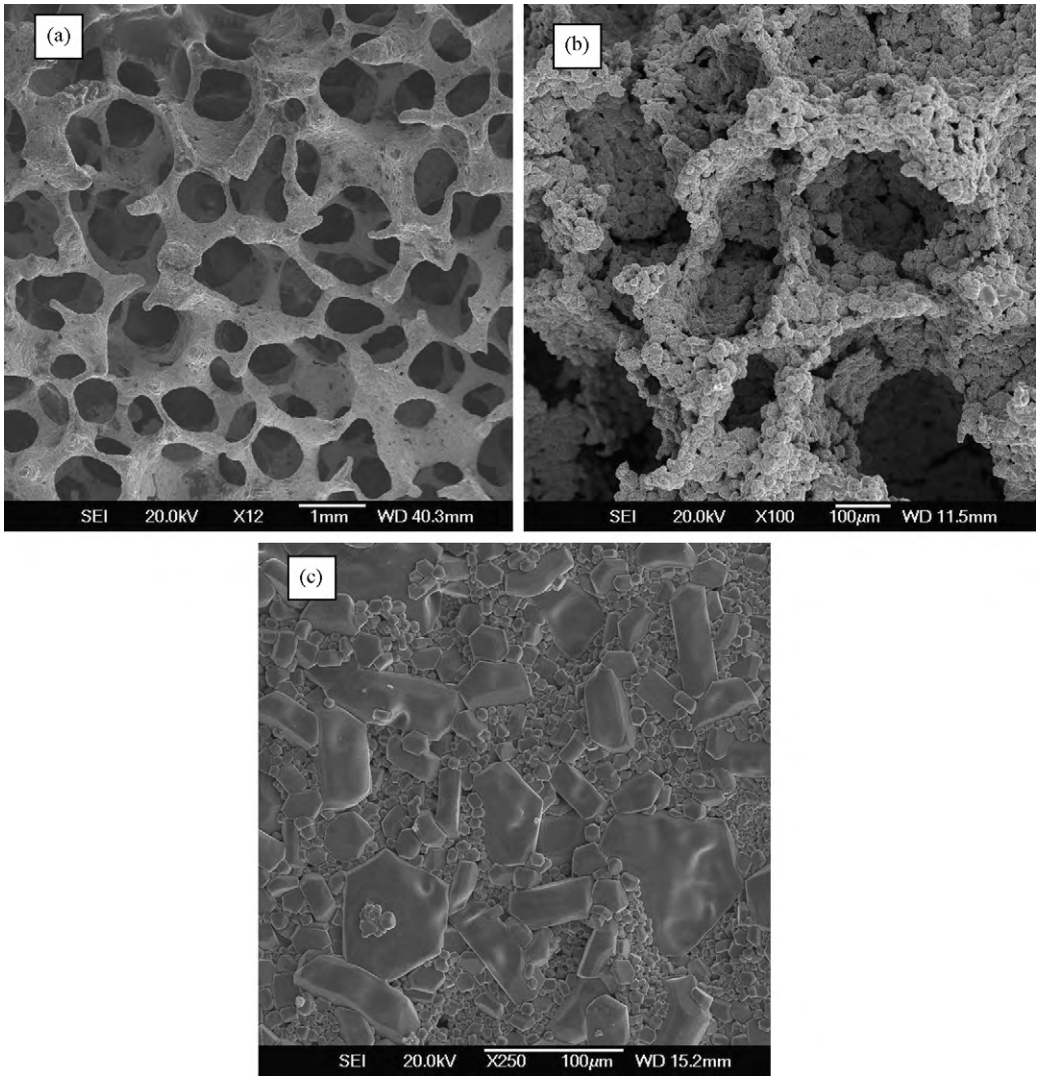

Fig. 2. SEM images of the foam samples having (a) 30 pores/in., (b) 80 pores/in. and (c) the compact samples.

fications), which is peculiar to the M-type of $BaFe_{12}O_{19}$ phase. Ideally, the basic pore structure of open celled foams is that of a dodecahedron. The actual pore structure is shown in the scanning electron microscope pictures of $BaFe_{12}O_{19}$ foams with 30 pores/in. and with 80 pores/in. (Fig. 2(a) and (b)). In all cases the pores were interconnected. The struts of the foams with 30 pores/in. do not show any surface cracks usually present in foams prepared from ceramic slurries.[13] Also the struts of the foams with 80 pores/in. show very few surface cracks. Such cracks are likely to be caused by non uniform coating of the polymeric foam by the ceramic slurry.[13,14] While pore diameters are between 0.5 mm and 1 mm in the sample of 30 pores/in., it ranges between 0.1 mm and 0.3 mm in the sample of 80 pores/in. Notice that there is almost no porosity in the compact sample. Densities of $BaFe_{12}O_{19}$ compact sample is 4.23 g/cm^3. The total porosity of $BaFe_{12}O_{19}$ foams with 30 pores/in. and 80 pores/in. samples were determined to be 90 vol% and 85 vol%, respectively.

Fig. 3 shows the *M–H* curves of the compact and the foam samples. It is seen that saturation magnetization M_s takes lower values at the foam samples compared to the compact one. On

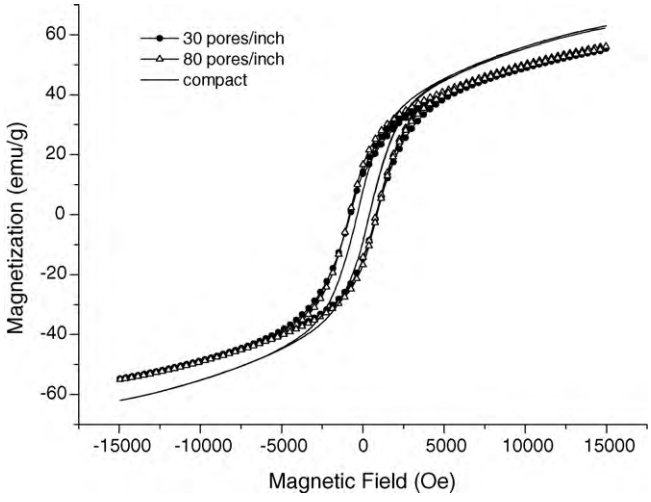

Fig. 3. The *M–H* curves of the foam and the compact samples.

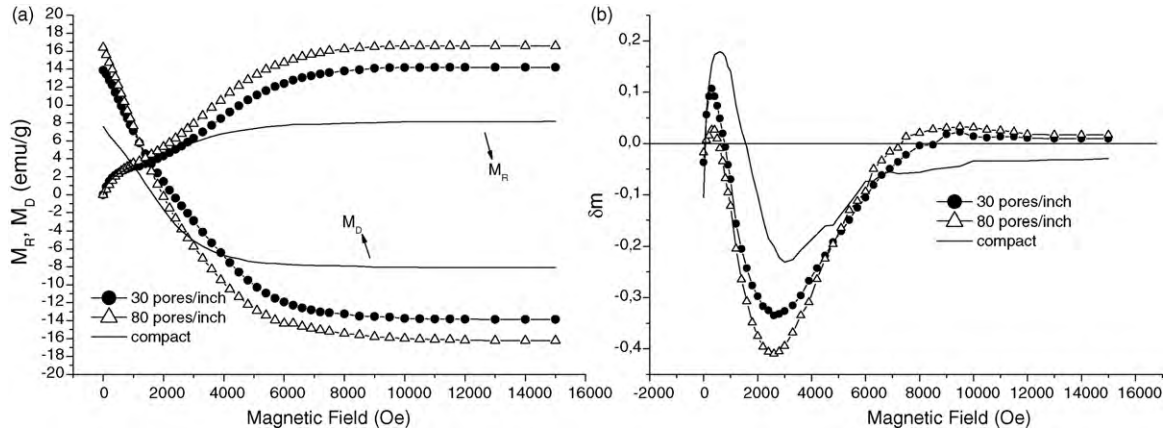

Fig. 4. (a) Isothermal magnetization remanence, $M_R(H)$, and demagnetization remanence, $M_D(H)$, curves and (b) δm plots as a function of magnetic field for the foam and the compact samples.

the other hand, coercivity becomes higher with the existence of porosity. The M_s values were determined to be 63.0, 55.5 and 55.1 emu/g for the samples compact, 80 pores/in. and 30 pores/in., respectively. As in the case of the M_s values, coercive fields are also almost same in the foam samples. Coercive fields were determined to be 850 Oe for the sample of 80 pores/in. and 800 Oe for the sample of 30 pores/in. Such differences observed on magnetic parameters are most probably due to the differences on the natures of interparticle interaction forces. Close-packed particles in the compact sample influence each other and make magnetic alignment under the field easier. On the other hand, presence of porosities in the samples of 80 pores/in. and 30 pores/in. prevent the exchange couplings between particles and thus, magnetic rotation realizes at higher fields, which causes higher coercivity, and resulting magnetization along the direction of field becomes smaller.

Isothermal magnetization remanence, $M_R(H)$, and demagnetization remanence, $M_D(H)$, curves are shown in Fig. 4(a). Foam samples have higher remanence magnetizations compared to the compact sample. The field at which saturation in remanences are seen also takes lower values in the compact one. Fig. 4(b) illustrates δm plots as a function of magnetic field. As seen, the δm takes both positive and negative values in all samples, which is different from the Wohlfarth expression for noninteracting particles in which horizontal line through the origin is expected.[11] The δm values first reach to maximum at positive side then changes sign and shows a secondary maximum at negative side in all samples. Above 7000 Oe, all curves converge to zero. This curvature is typical for all samples, which is independent of the porosity. However, the points where maximums seen differ with the porosity. For instance, 300 Oe, 350 Oe and 600 Oe are the fields at which positive maximums are seen for the samples of 30 pores/in., 80 pores/in. and the compact one, respectively. Similar arrangement is also seen at negative side. Negative maximums are at 2600 Oe for the samples of 80 pores/in. and 30 pores/in., but it is at 3000 Oe for the compact one. In other words, the field values of maximum points are almost same for the porous samples and it increases with the removal of porosity. Besides, the maximum values of δm also show variations depending on the amount of porosity, as shown in Fig. 4(b). Magnitude of the positive δm peak is the highest at the compact sample. This can be interpreted as an increase in resistance to the magnetization reversal in increasing reversing fields with the decrease of porosity (or reduction in this resistance with the increase of porosity). On the other hand, the highest δm value belongs to the sample of 80 pores/in. at negative side. It also confirms the reduction in the resistance against magnetization reversal with the porosity. It will be also informative to notice that these values of δm are comparable to those found in hard disks, tapes and floppy disks.[5,15,16]

Patel et al. has shown that the δm plots for the powder samples are negative for all fields.[17]

On the other hand, we have recently shown that the δm may take both positive and negative values even for powder samples if the grains are in single domain limit and the secondary phases are existent in addition to the main $BaFe_{12}O_{19}$ phase.[18] Studied samples are neither in single domain limit nor including impurity phases. That is, bulk natures of the studied samples may be the reason of observed positive and negative plots. One of the important outputs of the δm plots is seen as negative region expands but positive region becomes narrower with presence of porosity. Negative δm values suggest that the interactions between particles are always demagnetizing.[4,5] This kind of interaction is known to destabilize remanence state since it assists the reversal mechanisms. Therefore, it will be correct to say that existence of porosities in the studied samples increases the strength of demagnetizing-like interactions of neighboring particles and tend to assist magnetization reversal. On the other hand, positive δm values are associated to the interparticle interactions which contribute to the magnetization constructively.[6–8] That is, it will enhance the remanence state. As a result, present study reveals that close-packed particles (compact sample) seem promoting the magnetization state more compared to the loosely packed ones (porous samples).

4. Conclusion

In the present study, we have investigated the effects of porosity on the magnetic properties of hard magnetic $BaFe_{12}O_{19}$ samples. Our measurements have shown that magnetic prop-

erties of the porous samples, such as coercivity and saturation magnetization, are suitable for their possible applications in different areas. Existence of the porosity is observed to increase the coercieve field while it decreases the saturation magnetization. The strength of demagnetizing-like interactions between particles seems to increase with the presence of porosity, thus the porosity tends to destabilizing the remanence state. Close-packed particles interact with each other which assist to the stabilization and the enhancement of the remanence state.

References

1. Wang S, Ng WK, Ding J. Preparation and characterization of Al doped longitudinal barium ferrite thin film media. *Scr Mater* 2000;**42**:861–5.
2. Paul KB. Magnetic and structural properties of Ba M-type ferrite-composite powders. *Physica B* 2007;**388**:337–43.
3. Topal U, Bakan HI. Permanently magnetic $BaFe_{12}O_{19}$ foams: synthesis and characterization. *Mater Chem Phys* 2010;**123**:121–4.
4. Zhang H, Rong C, Du X, Zhang J, Zhang S, Shen B. Investigation on intergrain exchange coupling of nanocrystalline permanent magnets by Henkel plot. *Appl Phys Lett* 2003;**82**:4098–100.
5. Garcia-Casillas PE, Beesley AM, Bueno D, Matutes-Aquino JA, Martinez CA. Remanence properties of barium hexaferrite. *J Alloys Compd* 2004;**369**:185–9.
6. Cui BZ, O'Shea MJ. Exchange coupling and magnetic properties of $Nd_2Fe_{14}B$/Co nanocomposite thin films. *J Magn Magn Mater* 2003;**256**:348–54.
7. Geshev J, Schmidt JE. Interaction fields evaluation in fine particle systems. *IEEE Trans Magn* 1997;**33**:2504–8.
8. El-Hilo M, Bsoul I. Interaction effects on the coercivity and fluctuation field in granular powder magnetic systems. *Physica B* 2007;**389**:311–6.
9. Skomski R, Coey JMD. Giant energy product in nanostructured two-phase magnets. *Phys Rev B* 1993;**48**:15812–6.
10. Hadjipanayis GC. Nanophase hard magnets. *J Magn Magn Mater* 1999;**200**:373–91.
11. Wohlfarth EP. Relations between different modes of acquisition of the remanent magnetization of ferromagnetic particles. *J Appl Phys* 1958;**29**:595–6.
12. Kelly PE, Grady KO, Mayo PI, Chantrell RW. Switching mechanisms in cobalt-phosphorus thin films. *IEEE Trans Magn* 1989;**25**:3881–3.
13. Vedula VR, Green DJ, Hellman JR. Thermal shock resistance of ceramic foams. *J Am Ceram Soc* 1999;**82**:649–56.
14. Brown DD, Green DJ. Investigation of strut crack formation in open cell alumina ceramics. *J Am Ceram Soc* 1994;**77**:1467–72.
15. Yamanaka K, Uesaka Y, Okuwaki T. Magnetic viscosity of oriented barium ferrite media. *J Magn Magn Mater* 1993;**127**:233–40.
16. Kodama N. Magnetic interactions and media nosie in rigid disks. *J Magn Magn Mater* 2001;**224**:113–23.
17. Patel V, El-Hilo M, O'Grady K, Chantrell RW. Fluctuation fields of reversal in oriented and non-oriented barium ferrite media. *IEEE Trans Magn* 1993;**29**:3622–4.
18. Topal U. Factors influencing the remanent properties of hard magnetic barium ferrites: impurity phases and grain sizes. *J Magn Magn Mater* 2008;**320**:331–5.